

Dynamic Viscoelasticities for Short Fiber–Thermoplastic Elastomer Composites

WUYUN GUO and MICHIO ASHIDA*

The Graduate School of Science and Technology, Kobe University, Nada, Kobe 657, Japan

SYNOPSIS

Dynamic moduli, E' and E'' , and loss tangent $\tan \delta$ were investigated for thermoplastic elastomers (TPEs), styrene–isoprene–styrene copolymers (SISs), styrene–butadiene–styrene copolymer (SBS), and Hytrel and composites reinforced by poly(ethylene terephthalate) (PET) short fibers. The styrenic TPEs have a typical rubbery behavior and the Hytrel TPE has medial characteristics between rubber and plastic. Both E' and E'' of the composites depended on the matrix as well as the fiber loading and fiber length. Based on the viewpoint of different extensibility between the fiber and the matrix elastomer, a triblock model was considered for estimating the storage modulus of the short fiber–TPE composites as follows: $E_c = \alpha V_f E_f + \beta(1 - V_f) E_m$, where α and β are the effective deformation coefficients for the fiber and the matrix elastomer, respectively. They can be quantitatively represented by modulus ratio $M (= E_m/E_f)$ and fiber length L : $\alpha = (L^n + k)M/(L^n M + k)$, $\beta = (1 - \alpha V_f)/(1 - V_f)$, where the constants n and k are obtained experimentally. When $k = 0.022$ and $n = 0.45$, E_c of the TPE composites agreed well with the prediction of the proposed model. The relaxation spectrum of the composites showed a distinct main peak ascribed to the matrix elastomer, but no peak to the PET fiber. The relative damping of main relaxation, $(\tan \delta_{\max})_c/(\tan \delta_{\max})_m$, decreased monotonously with increasing fiber loading and fiber length and with decreasing modulus of matrix elastomer. Thus, the relative damping may be attributed not only to the volume effect of matrix, but also to the unevenness of the strain distribution in the matrix phase, which depends on the fiber length and the matrix's modulus. The findings prove that the different extensibility between fiber and matrix and the uneven distribution of strain in matrix were important for the short-fiber reinforcement of the TPE composites. © 1993 John Wiley & Sons, Inc.

INTRODUCTION

Elastomer composites reinforced by short fiber combine the elasticity of the matrix with the strength and stiffness of the reinforcing fiber.¹ Short-fiber reinforcement of the matrix elastomer increases modulus and strength and decreases ultimate elongation and swelling.^{2–5} In previous papers,^{6,7} the mechanical properties have been discussed for two types of thermoplastic elastomer (TPE; styrenic and polyester TPEs) composites reinforced by PET short fibers. It was found that the stress–strain behavior of the composites was affected by the me-

chanical properties of the TPE matrix, which depended mainly on a ratio of hard and soft segments in the matrix elastomer. It was also found that the continuous matrix phase and the rigid phase of fibers in the composite exhibited different deformation behaviors: The matrix elastomer underwent the most deformation of the composite, whereas the fiber adsorbs large internal stress with little deformation.

The dynamic moduli, E' and E'' , and mechanical damping, $\tan \delta$, of the organic short fiber–rubber composites have been investigated as a function of temperature by a Rheovibron.⁸ In the longitudinal direction of fibers, E' increases monotonously with increasing fiber length and shows a linear relationship with fiber loading. The modulus data of the short fiber–rubber composites could not be predicted well by the general empirical rules.^{9–11} This was con-

* To whom correspondence should be addressed.

sidered to be due mainly to neglecting the low modulus of the elastomer matrix and its high elasticity.⁷

In the present paper, the dynamic moduli and loss tangent for the PET short fiber–thermoplastic elastomer composites were investigated, and the micromechanics for estimating moduli were considered by using a block model for describing quantitatively the behavior of the modulus.

EXPERIMENTAL

Materials

The thermoplastic elastomers (TPEs) used were styrenic block copolymers of two styrene–isoprene–styrene copolymers (SISs) with different styrene contents and one styrene–butadiene–styrene copolymer (SBS) (Shell Co., Ltd.) and a poly(ether ester) thermoplastic elastomer (trade name Hytrel TR2300, abbreviated as Hytrel, DuPont). Their properties are given in Table I. The short fiber used was poly(ethylene terephthalate) (PET) with various lengths as given in Table I (Teijin Co.).

Surface Treatment of PET Fiber

According to the surface treatments reported in previous papers,^{6,7} PET fibers were dipped in toluene solution that contained 2 wt % isocyanate and 3 wt % styrenic copolymer TPEs and were baked at 175°C for 3 min for the styrenic copolymer composites. For Hytrel composites, PET fibers were

dipped in a toluene solution that contained 5 wt % isocyanate and were baked at 115°C for 30 min.

Processing

The matrix TPEs and short fibers were mixed directly on an open roll with a 2 mm opening. The milling of compounds was always kept to the same direction in order to orient the fibers along the rolling direction in sheets. Finally, each stock was passed through the mill and then compressed at 150 and 130°C for the styrenic copolymer and Hytrel composites, respectively, for 15 min to form sheets that are 1.0 mm in thickness.

Measurement of Viscoelastic Properties

Dynamic viscoelasticities of the composites were measured along the fiber axis direction by a DVE-V4 FT Rheovibron (DVE Co.) that applied a sinusoidal tensile strain to the specimen. The measurements were carried out in the temperature range from –80 to 160°C with a heating rate of 2.0°C/min and at a frequency of 110 Hz with a strain amplitude of 0.015%.

THEORY OF MICROMECHANICS

In the previous papers,^{6,7} the different extensibility between fiber and matrix was considered as an important reinforcement factor for the short fiber–TPE composites. This viewpoint has been introduced into the parallel model to predict the mechanical properties of the composites. On the other hand, a coupling arrangement of the block model has been discussed by Bauer and Crossland¹² to represent different extensibility of each constituent in carbon-black-loaded elastomers. In the present study, the block model is considered for estimating the moduli of the short fiber–elastomer composites, corresponding to the unevenness of deformation in the composite.

Figure 1(1) is a schematic representation of uniaxially oriented short fiber–elastomer composite that shows the distributive state of the fibers (as phase “*f*”) in the matrix elastomer (as phase “*m*”). Figure 1(2) is the equivalent model of the composite in Figure 1(1). The fiber and the matrix elastomer are completely bonded to each other.

When such a sample of the composite in Figure 1(1) is elongated in the fiber direction, the elastomer matrix is subjected mainly to deformation that is not uniform due to the fiber loading. In general, the

Table I Thermoplastic Elastomers and Short Fibers

Elastomer	Density (g/cm ³)	Hardness (Shore A)	Styrene/ Elastomer (wt %)
SIS(1) (TR1107)	0.92	37	14/86
SIS(2) (TR1111)	0.93	52	21/79
SBS (TR1024)	0.94	59	42/58
Hytrel (TR2300)	1.17	32	—

	Diameter (mm)	Length (mm)
PET short fibers	0.028	0.5
		2.0
		4.0
		6.0

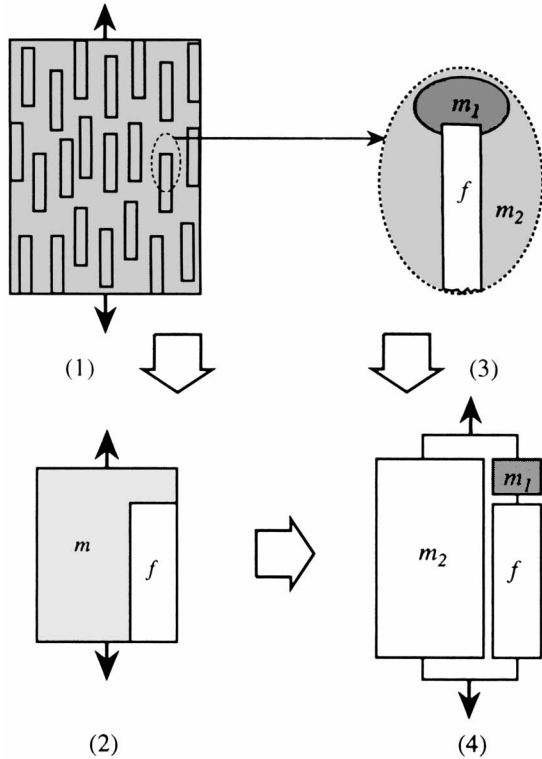


Figure 1 Block models for fiber filler-matrix model.

area surrounding the fiber's end undergoes much larger deformation than that surrounding the fiber's center, as shown in Figure 1(3). Taking the above circumstance into consideration, a simple mechanical model is applied for calculating the moduli of the equivalent model in Figure 1(2). Figure 1(4) shows the mechanical triblock model, which is analogous to Takayanagi's "parallel sea-island" model.¹³ This model is a parallel arrangement consisting of a matrix phase (m_2) and a series coupling (f, m_1) that has a modulus of E_1 . In physical significance, the m_1 phase represents the large deformation area of the matrix surrounding the fibers' end, and the m_2 is the other area of the matrix, which has a small deformation constrained by the fibers. If E_f and E_m are the moduli of fiber and the matrix elastomer, and V_f, V_{m_1} , and V_{m_2} are the volume fractions of the f, m_1 and m_2 , respectively, the composite modulus E_c under a small extension condition can be written using the simple rule of mixtures as follows:

$$E_c = (V_f + V_{m_1})E_1 + V_{m_2}E_m, \quad (1)$$

$$\frac{(V_f + V_{m_1})}{E_1} = \frac{V_f}{E_f} + \frac{V_{m_1}}{E_m}, \quad (2)$$

where $V_{m_1} + V_{m_2}$ is equal to the volume fraction of

the matrix elastomer and $V_f + V_{m_1} + V_{m_2} = 1$. From eqs. (1) and (2), E_c can be represented as

$$E_c = \alpha V_f E_f + \beta (1 - V_f) E_m \quad (3)$$

where

$$\alpha = \frac{(V_f + V_{m_1})M}{V_f M + V_{m_1}} \quad (4a)$$

$$\begin{aligned} \beta &= \frac{(V_f M + V_{m_1}) - V_f M (V_f + V_{m_1})}{(V_f M + V_{m_1})(1 - V_f)} \\ &= \frac{1 - \alpha V_f}{1 - V_f} \end{aligned} \quad (4b)$$

where M is the moduli ratio (E_m/E_f). Equations (3) and (4b) show the same expressions as shown in the previous paper.⁷ Therefore, α and β , the effective deformation coefficients for fiber and the matrix elastomer, respectively, also give the meaning of the effective reinforcement of the short fiber.

In eq. (4a), V_{m_1} can be assumed to be proportional to the number of fiber ends in unit volume, $2N_f$, and to the power of the fiber length, L^s , namely,

$$\begin{aligned} V_{m_1} &= k'(2N_f)L^s \\ &= k'[8V_f L^s / (\pi d^2 L)] \\ &= kV_f / L^n \end{aligned} \quad (5)$$

where N_f is the number of fibers in unit volume; d , the diameter of the fiber; s and n ($= 1 - s$), the experimental constants; and k' and k ($= 8k'/\pi d^2$), the proportional coefficients. Finally, α can be represented by substituting V_{m_1} into eq. (4a) as

$$\alpha = \frac{L^n + k}{L^n M + k} M \quad (6)$$

Obviously, the α in eq. (6) does not depend on V_f and monotonously increases with increasing L when M is much smaller than 1.

RESULTS AND DISCUSSION

Dynamic Moduli

Dynamic moduli of composites depend on matrix type, fiber loading, and fiber length. Storage moduli, E' , of SIS (1), SIS (2), SBS, and Hytrel composites are shown as a function of temperature in Figure 2. The E' s of the SIS (1) and SIS (2) composites fall

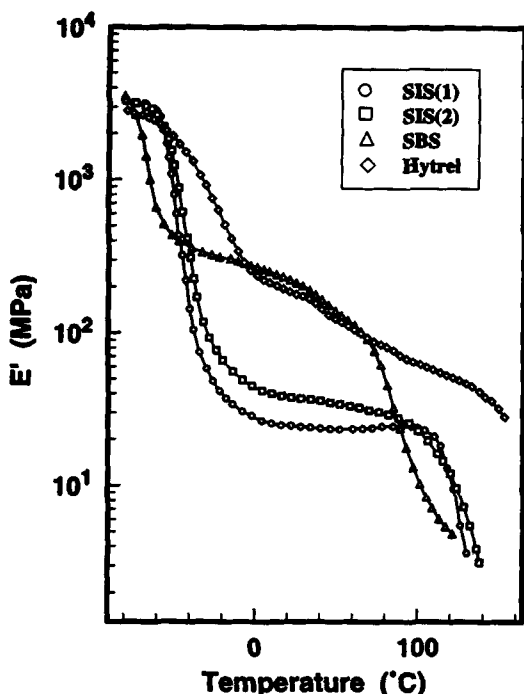


Figure 2 Temperature dependences of E' for SIS(1), SIS(2), SBS, and Hytrel composites filled with 10 vol % fibers that are 6 mm in length.

steeply at about -50°C to almost a plateau at a different level over the temperature range from 0 to 90°C , followed by the second drop above 90°C . The curves show typical rubbery behavior like their matrix elastomers. The first drop in E' at low temperatures is due to the glass transition, and the second one at high temperatures is due to melting of the TPE materials; in between is the rubbery plateau region.¹⁴ The SBS composite shows the rubbery plateau region between -15 and 70°C , located at a lower temperature than that of the SIS composites. The E' values at the rubbery plateau region increase in the order of the composites of SIS(1), SIS(2), and SBS. The E' of the Hytrel composite decreases gradually with rising temperature. The rubbery region is at temperatures above 4°C , but its E' drops after an inflection at about 35°C . All the composites displayed similar dependence of E' on temperature to that of the respective matrix elastomers in the rubbery region.

The effect of fiber loading was observed on temperature dependence of E' and E'' for the SIS(1) composites filled with fiber of 6 mm in length, as shown in Figure 3. E' depends little on fiber loading in the glassy state and increases greatly with increasing fiber loading in the rubbery plateau region, but the increment becomes small with over 10 vol

% fiber. In addition, the curves of E' in the rubbery state become flatter and the rubbery range extends to the higher-temperature side when fiber loading increases, which suggests that the thermal stability of elasticity for the SIS(1) elastomer is improved by fiber loading. A sharp peak in E'' corresponding to the glass transition appears at about -56°C and its height and position vary little with fiber loading. In the rubbery state, E'' as well as E' increase with increasing fiber loading and increase gradually with rising temperature, although the matrix elastomer has a constant E'' value. The dependence of E' on fiber loading for the SIS(2) and SBS composites showed a similar tendency to that for SIS(1) composites.

The effect of fiber length on E' and E'' for the Hytrel composites containing 10 vol % fiber is shown in Figure 4. The E' values increase a little in the glassy state and much more in the rubbery state with increasing fiber length, which is similar to the effect of the fiber loading. The increment of increase in E' in the rubbery state becomes small when fiber length is longer than 2 mm. In addition, the E' curve of the composite filled with fiber of 0.5 mm length shows a similar tendency to that of the matrix elastomer and has a higher value than the latter in the rubbery region. The curves of the composites filled

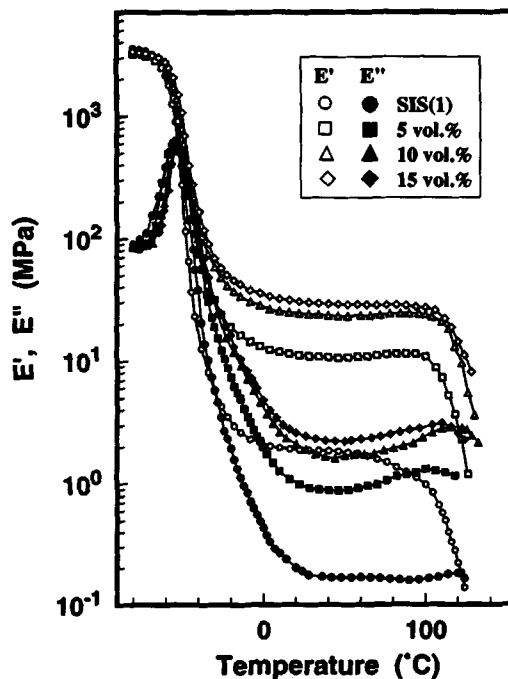


Figure 3 Effect of fiber loading on E' and E'' dependence on temperature for SIS(1) composites filled with fiber that is 6 mm in length.

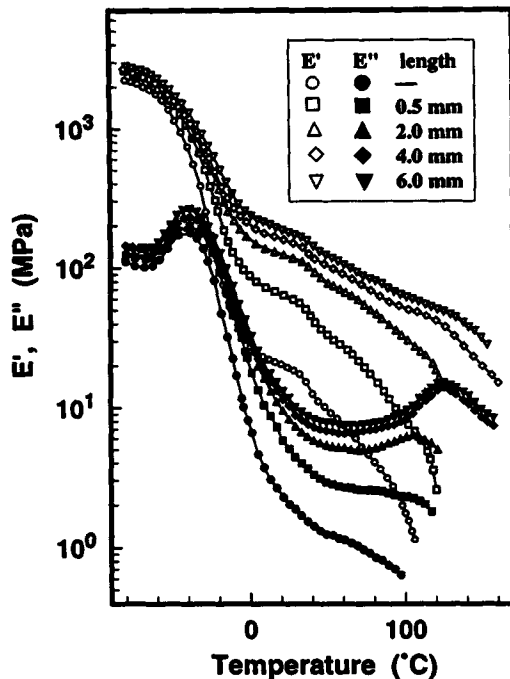


Figure 4 Effect of fiber length on E' and E'' dependence on temperature for Hytrel composites filled with 10% fibers.

with fiber of length over 2 mm become flatter above 35°C compared to the matrix elastomer, which implies that the thermal stability of elasticity of Hytrel is also improved when fiber length is increased. These results confirm that fiber length of 2.0 mm is a critical length for reinforcement of the composite. On the other hand, E'' of the Hytrel composite shows the glass transition peak at about -38°C, and its intensity increases with increasing fiber length. As in the case of E' , E'' in the rubbery region increases with increasing fiber length and E'' increases greatly at temperatures above 80°C.

To investigate E' of the composites in the rubbery plateau region, the E' value at 20°C was plotted as a function of matrix type, fiber loading, and fiber length, and the prediction of eq. (3) was considered with a value of fiber modulus ($E_f = 5.8$ GPa). Figure 5 shows the relationships between E' and fiber loading for SIS(1), SIS(2), SBS, and Hytrel composites. E' increases monotonously with increasing fiber loading as does Young's modulus.^{6,7} E' increases steeply for the SBS and Hytrel composites and gradually for the other cases. The lines in the figure are given by eq. (3). It seems that the predictions of eq. (3) agree well with the experimental results of each composite so long as the values of α are properly chosen. When the fiber is loaded more than

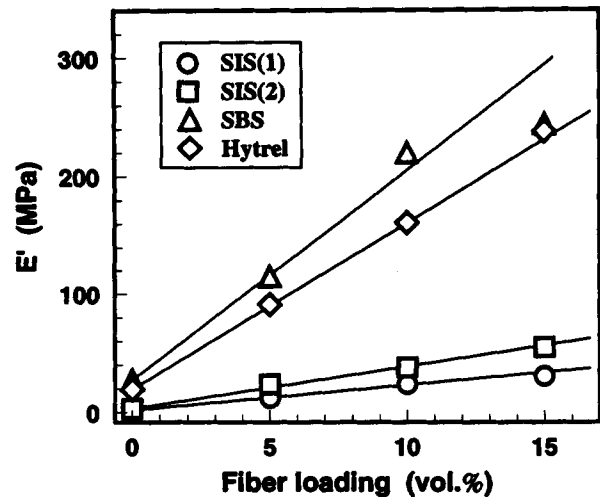


Figure 5 Effect of fiber loading on E' at 20°C for SIS(1), SIS(2), SBS, and Hytrel composites. The predicted lines were drawn from eq. (3).

15 vol %, the E' obtained is off the predicted lines, which may be due to the poor orientation of fiber in the composites.⁷ Furthermore, the effect of fiber length on E' of the SIS(1) and Hytrel composites are shown in Figures 6 and 7, respectively. The E' s increase monotonously with increasing fiber loading and the slopes become steeper with increasing fiber length for both SIS(1) and Hytrel composites. The lines given by eq. (3) agree well with the experimental results by using the chosen α values.

With the various values of α obtained above, we can further examine the prediction of eq. (6). Figure 8 describes the relationship between α and modulus

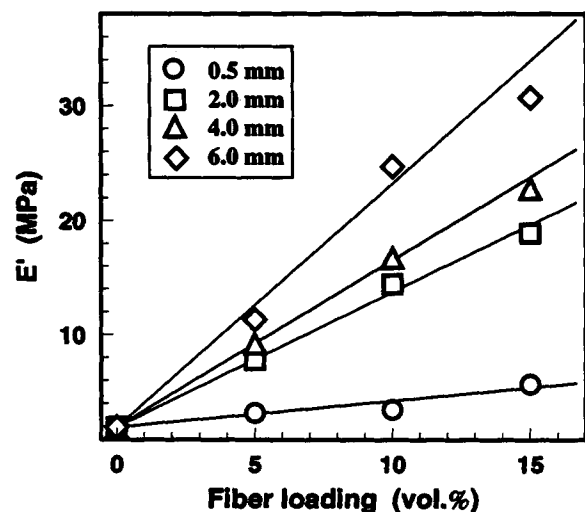


Figure 6 Effect of fiber length on E' at 20°C for SIS(1) composites. The predicted lines were drawn from eq. (3).

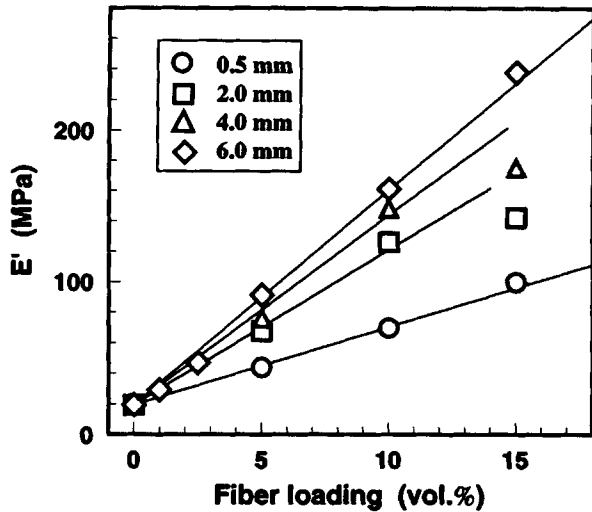


Figure 7 Effect of fiber length on E' at 20°C for Hytrel composites. The predicted lines were drawn from eq. (3).

ratio $M (= E_m/E_f)$, which shows a monotonous increase of α with M . When $k = 0.022$ and $n = 0.45$, eq. (6) coincides well with the plots of α . Figure 9 shows the dependence of α on the fiber length for the SIS(1) and Hytrel composites. Obviously, α is a monotonous incremental function of fiber length. The curves in the figure were drawn from eq. (6) by giving the same k and n values as those obtained from Figure 8 and coincide well with the experimental data. This fact indicates that k and n are constants for the present TPE composites and that the modified parallel model can describe very well the behavior of modulus for the TPE composites reinforced by short fiber. Based on eq. (6), α in-

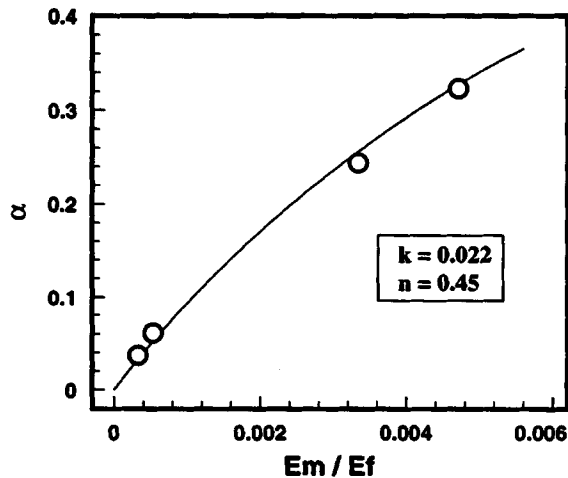


Figure 8 Dependence of α on modulus ratio (E_m/E_f) for TPE composites. The line was drawn from eq. (6).

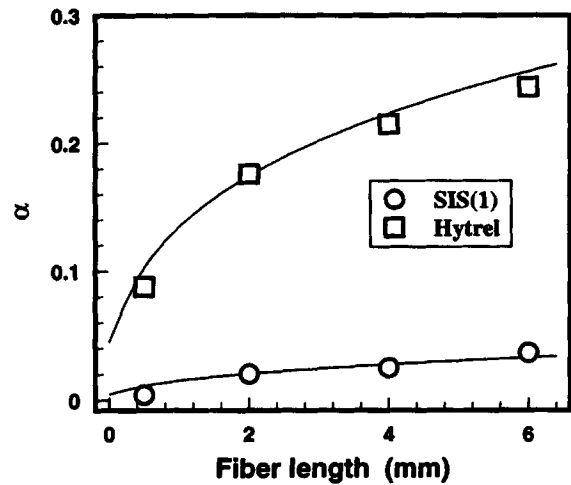


Figure 9 Dependence of α on fiber length for SIS(1) and Hytrel composites. The lines were drawn from eq. (6), in which $k = 0.022$ and $n = 0.45$.

creases monotonously with increasing M and approaches unity when $M = 1$, and α increases with increasing fiber length and approaches unity if the fiber is very long. When $\alpha = 1$, the modified parallel model becomes the general parallel model that is used in long-fiber composites. The results obtained indicate that the different extensibility between fiber and matrix is the most important factor for short-fiber reinforcement of the TPE composites.

Figure 10 shows the effect of tensile angle θ to the fiber orientation on E' at 20°C for SIS(1),

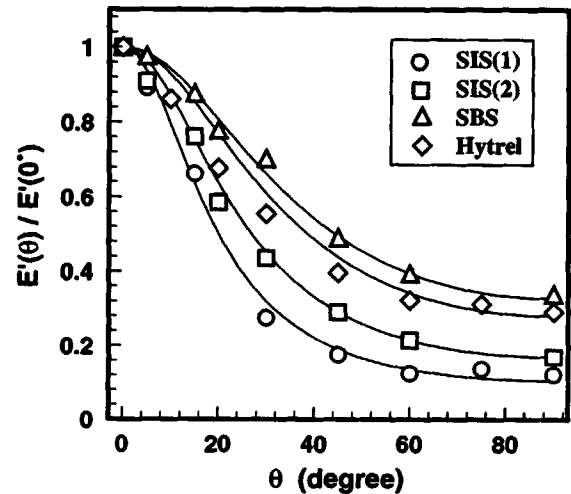


Figure 10 Effect of fiber orientation on E' for SIS(1), SIS(2), SBS, and Hytrel composites loaded 10 vol % fibers that are 6 mm in length. The lines are drawn from Coran's equation.

SIS(2), SBS, and Hytrel composite filled with 10 vol % fiber of 6 mm in length. The E' falls steeply when θ is small, whereas it decreases gradually above 45° . The E' in the transverse direction depends on matrix type and decreases in the order of SBS, SIS(2), Hytrel, and SIS(1). The lines in the figure are drawn with Coran's equation as follows¹⁵:

$$\frac{1}{E'(\theta)} = \frac{\cos^2(\theta)}{E'(0^\circ)} + \frac{\sin^2(\theta)}{E'(90^\circ)} \quad (7)$$

where $E'(0^\circ)$ and $E'(90^\circ)$ are the moduli at the longitudinal and transverse direction to the fiber orientation, respectively. Obviously, the predictions by eq. (7) are good for the experimental results of the styrenic TPE composites, which clearly suggests that the orientation of fiber is well controlled in the composites with 10 vol % fiber.

Relaxation Spectrum

The relaxation spectra of composites in the transition region depend mainly on the mechanical relaxation of the matrix and loaded fiber and are affected to different extents by the interface between fiber and matrix and between the fiber loading and length. It has been reported⁸ experimentally that the $\tan \delta$ of the rubber composites showed two dispersion peaks: one at a low temperature corresponding to the main dispersion of the matrix rubber and the other at a high temperature due to the main dispersion of the loaded fibers. In addition, a small

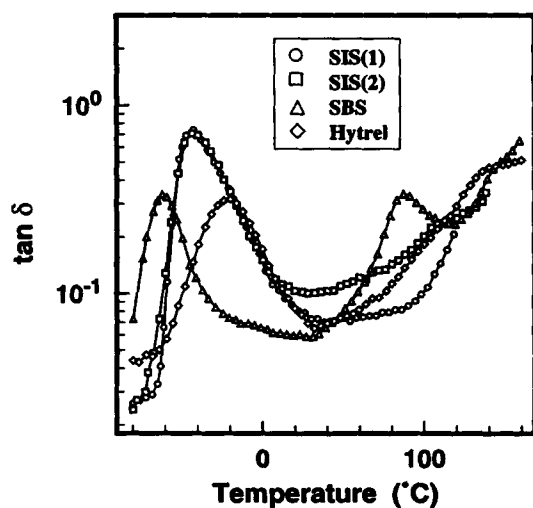


Figure 11 Temperature dependence of $\tan \delta$ for SIS(1), SIS(2), SBS, and Hytrel composites filled with 10 vol % fibers that are 6 mm in length.

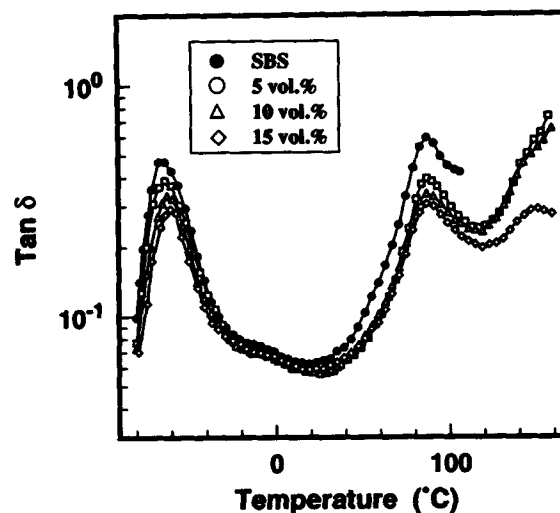


Figure 12 Effect of fiber loading on temperature dependence of $\tan \delta$ for SBS composites loaded fiber that is 6 mm in length.

and broad peak was observed between the two peaks that was considered to be due to the interface region in the composite. On the other hand, the main relaxation has a tendency to decrease in height with increasing fiber loading.^{8,16,17}

Figure 11 shows the temperature dependence of $\tan \delta$ for the SIS(1), SIS(2), SBS, and Hytrel composites filled with 10 vol % fiber that is 6 mm in length. Within the experimental range, $\tan \delta$ of the composites was similar to those of the respective matrix elastomers. The main peaks of the composites are lower and broader than those of the respective elastomers and are due to the glass transition of the soft domain in the matrix elastomer. On the other hand, a peak at higher temperature is observed at about 86°C for the SBS composite, which is considered to be due to the glass transition of the styrenic hard domain of the matrix SBS. The same peak, however, does not clearly appear in the case of the SIS composites, which may be due to insufficient styrene content in the matrix SIS. On the other hand, it is well known that PET fiber has a main relaxation ascribed to micro-Brownian motion of amorphous chains and a second relaxation due to the rotation of local bonds in the main chains.¹⁸ In the temperature range of this study, both main and second relaxations do not appear obviously as maxima in $\tan \delta$. They may be covered by the melting peak for the elastomer and the main relaxation of the soft domain in the elastomer. Figure 12 shows the effect of fiber loading on $\tan \delta$ for the SBS composites filled with fiber of 6 mm in length. The maximum value at the main relaxation decreases with

increasing fiber loading. The peak at high temperature has a similar tendency to the main relaxation.

To investigate the effect of short-fiber reinforcement of TPE elastomer on main relaxation, the relative damping of $\tan \delta$ for the composites to the corresponding elastomer, $(\tan \delta_{\max})_c / (\tan \delta_{\max})_m$, was plotted as a function of TPE type, fiber loading, and fiber length. Figure 13 shows the effect of fiber loading and TPE type. The relative damping drops steeply at the low fiber loading and decreases gradually over 10 vol % fiber loading, which has no obvious linear relationship with the fiber loading although the PET-chloroprene rubber composites show the linear relationship described in previous paper.⁸ On the other hand, the relative damping of composites increases in the order of SIS(1), SIS(2), Hytrel, and SBS, corresponding to increasing modulus of the matrix elastomer. Figure 14 shows the effect of the fiber length on the relative damping for the SIS(1) composites. The relative damping decreases monotonously with increasing fiber length, but its decrease rate becomes smaller when the fiber length is longer than 2 mm.

The maximum for main relaxation is usually related to the volume fraction of the matrix phase. However, it is difficult to explain the dependence of

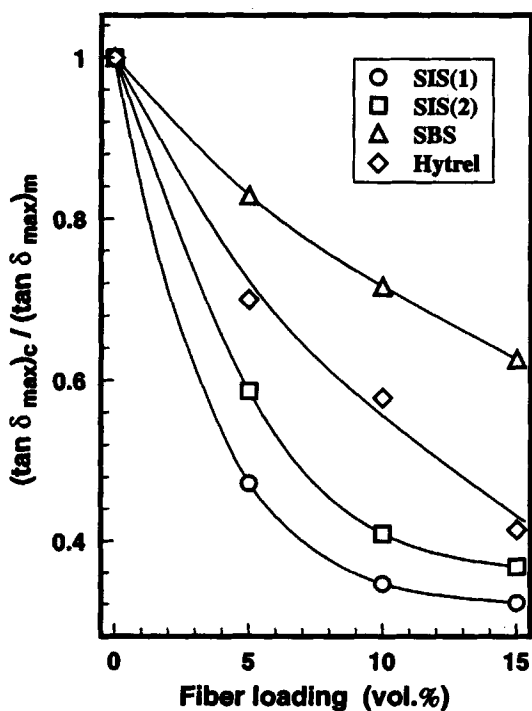


Figure 13 Effect of fiber loading on relative damping at the maximum of $\tan \delta$ for SIS(1), SIS(2), SBS, and Hytrel composites filled with fiber that is 6 mm in length.

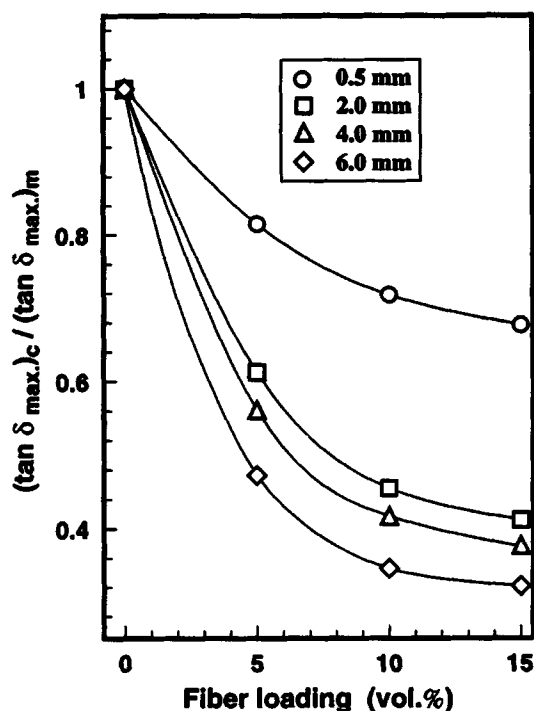


Figure 14 Effect of fiber length on relative damping at the maximum of $\tan \delta$ for SIS(1) composites.

the relative damping on matrix type and fiber length from only the volume effect. In fact, an uneven distribution of strain in the matrix phase is also important in its affect on the reinforcement of composites, and the unevenness occurs mainly between the matrix around a fiber's end and that surrounding a fiber's center. Thus, it seems that the damping of the composites also depends on the uneven distribution of strain in the matrix phase as well as on the volume effect. For the short fiber-TPE composites, the uneven distribution of strain in the matrix may be more important to control the damping, because both the decrease of the modulus ratio (E_m/E_f) and the increase of fiber length can give rise to more uneven distribution of the strain in the matrix phase.

CONCLUSION

The dynamic mechanical properties are generally described by both moduli, E' and E'' , and loss tangent, $\tan \delta$. The short fiber-TPE composites show the obvious reinforcement effect of the short fiber in the magnitude of E' in the rubbery plateau region, and E' increases in the order of SIS(1), SIS(2), Hytrel, and SBS with increasing fiber loading and

length. Both E' and E'' at high temperature increase with fiber loading for the SIS(1) and Hytrel composites as compared with the matrix elastomers, whereas they do not increase for the SIS(2) and SBS composites. The relaxation spectra of the TPE composites are controlled mainly by the properties of the matrix elastomer. From the dependence of $(\tan \delta_{\max})_c / (\tan \delta_{\max})_m$ on the matrix types, fiber loading, and fiber length, it is considered that the relative damping of the composites is attributed not only to the volume effect of the matrix phase, but also to the unevenness of the strain distribution in the matrix that was caused by the loaded fibers. These findings indicate that the TPE composites have different dynamic properties from the conventional thermosetting rubber composites and are controlled strongly by the matrix phase.

A triblock model was considered for estimating the modulus of the short fiber-TPE composites as follows:

$$E_c = \alpha V_f E_f + \beta(1 - V_f) E_m$$

where α and β are the effective deformation coefficients for the fiber and the matrix elastomer, respectively, and they can quantitatively be represented by moduli ratio $M (= E_m/E_f)$ and fiber length L :

$$\alpha = \frac{L^n + k}{L^n M + k} M, \quad \beta = \frac{1 - \alpha V_f}{1 - V_f}$$

where constants n and k are obtained experimentally.

When $k = 0.022$ and $n = 0.45$, E' of the TPE composites agreed well with the prediction of the model. This proves that the viewpoint about different extensibility between fiber and matrix is important to account for the short-fiber reinforcement of the TPE composites.

REFERENCES

1. L. A. Goettler and S. K. Shen, *Rubber Chem. Technol.*, **56**, 619 (1983).
2. V. M. Murty and S. K. De, *Rubber Chem. Technol.*, **55**, 287 (1982).
3. A. Y. Coran, K. Boustany, and P. Hamed, *Rubber Chem. Technol.*, **47**, 396 (1974).
4. T. Noguchi, M. Ashida, and S. Mashimo, *Jpn. Gomu Kyokaishi*, **56**, 768 (1983); **57**, 171 (1984); **57**, 829 (1984).
5. M. Ashida and T. Noguchi, *Compos. Polym.*, **2**, 339 (1989).
6. M. Ashida and W. Guo, *J. Appl. Polym. Sci.*, to appear.
7. W. Guo and M. Ashida, to appear.
8. M. Ashida, T. Noguchi, and S. Mashimo, *J. Appl. Polym. Sci.*, **29**, 661 (1984); **29**, 4107 (1984); **30**, 1011 (1985).
9. H. L. Cox, *Br. J. Appl. Phys.*, **3**, 72 (1952).
10. J. C. Halpin, *J. Elastoplast.*, **3**, 732 (1979).
11. J. C. Halpin and J. L. Kardos, *J. Appl. Phys.*, **43**, 2235 (1972).
12. R. F. Bauer and A. H. Crossland, *Rubber Chem. Technol.*, **63**, 779 (1990).
13. M. Takayanagi, *Mem. Fac. Eng. Kyushu Univ.*, **33**(1), 41 (1963).
14. J. C. West, and S. L. Cooper, in *Science and Technology of Rubber*, F. R. Eirich, Ed., Academic Press, New York, 1978, Chap. 13.
15. A. Y. Coran, K. Boustany, and P. Hamed, *J. Appl. Polym. Sci.*, **15**, 2471 (1971).
16. J. L. Gomez et al., *J. Appl. Polym. Sci.*, **42**, 1647 (1991).
17. K. Isaka and K. Shibayama, *J. Appl. Polym. Sci.*, **22**, 1321 (1978).
18. J. H. Dumbleton and T. Murayama, *Kolloid Z. Z. Polym.*, **220**, 41 (1967).

Received October 27, 1992

Accepted February 23, 1993